Data Classification, Visualization, and Enhancement Using n-Dimensional Probability Density Functions (nPDF): AVIRIS, TIMS, TM, and Geophysical Applications*

Abstract

The n-Dimensional Probability Density Functions (nPDF) approach is a user-interactive image analysis technique which overcomes many of the inherent limitations of traditional classifiers. In this paper we illustrate the applications of nPDF analysis in three broad areas: data visualization, enhancement, and classification. For data visualization, nPDF provides a method for transforming multiple bands of data in a predictable and scene-independent way. These transformations may be designed so as to enhance a particular cover type, or to give the best visual representation of the multiband image data. These approaches are illustrated with the enhancement of hydrothermally altered areas in Thematic Mapper (TM) data, and the display of a false-color composite of six bands of Thermal Infrared Multispectral Scanner (TIMS) imagery. Spectral frequency plots of the nPDF components give a multispectral view of data distribution that can be used to investigate the number and distribution of spectral classes in a high dimensional data set. In addition, these plots are used in a non-parametric classification of the image for discrimination of discrete classes, as well as for classes that are mixtures at the sub-pixel scale. In a mixed deciduous and coniferous forest, an nPDF Deciduous Forest Index shows a high correlation with percent deciduous vegetation determined from field surveys. A classification of TIMS imagery of Death Valley results in excellent discrimination of 13 discrete rock types. Classification of TM data, as well as classification of combined geophysical data, is used to illustrate the power and variety of complex applications. The procedure is the opposite of a "black box" approach: nPDF transformations and plots show graphical representations of the spectral and informational class distributions, and the user decides on the exact location of the spectral boundaries of each class in the classification. In comparisons with standard statistical classifiers, nPDF is extremely accurate and fast, making it possible to analyze large data sets, such as full scenes of Advanced Visible/Infrared Imaging Spectrometer (AVIRIS) data, on a personal computer.

Introduction

The n-Dimensional Probability Density Functions (nPDF) is a new, highly user-interactive approach to image processing. The technique has applications throughout the procedure of data display, enhancement, analysis, and classification. nPDF is both very fast and highly effective, making it ideal for processing high dimensional data such as Thematic Mapper (TM) or Airborne Visible/Infrared Imaging Spectrometer (AVIRIS) imagery on a personal computer. In this paper we illustrate the broad application and versatility of the approach using multiple data sets: TM data of known hydrothermally altered areas in Lincoln County, Nevada; six-band Thermal Infrared Multispectral Scanner (TIMS) data of Death Valley; correlation maps of gravity and magnetic data of Lincoln County, Nevada; AVIRIS data of Maricopa, Arizona; and TM data of Northwestern Ontario, Canada (see Figures 1 and 2 for location maps of the test sites.)

Commonly used classification techniques, such as maximum likelihood and Mahalanobis, have a number of inherent limitations. These limitations include: (1) The memory requirements of the computer routines tend to be very large for high dimensional data, and the run-times are very long; therefore, the algorithms tend to be implemented in computer routines that allow for only a limited number of input bands. (2) The algorithms are relative classifiers, and thus training fields from all spectral classes need to be identified prior to classification. Classes are described statistically; therefore, it is very difficult to check if the training fields selected represent the entire data. (3) Class overlap, class distribution, and interclass distances can be shown for only two bands at a time. Furthermore, interclass distances can be

*Presented at the Ninth Thematic Conference on Geologic Remote Sensing, Pasadena, California, 8-11 February 1993.

Photogrammetric Engineering & Remote Sensing, Vol. 59, No. 12, December 1993, pp. 1755–1764.

0099-1112/93/5912–1755$03.00/0
©1993 American Society for Photogrammetry and Remote Sensing

Haluk Cetin[1]
Department of Earth and Atmospheric Sciences, Purdue University, West Lafayette, IN 47907-1397
Timothy A. Warner
Department of Geology and Geography, West Virginia University, P. O. Box 6300, Morgantown, WV 26506-6300.
Donald W. Levandowski
Department of Earth and Atmospheric Sciences, Purdue University, West Lafayette, IN 47907-1397.

[1]Presently with the Indiana Geological Survey, 611 North Walnut Grove, Bloomington, IN 47405.

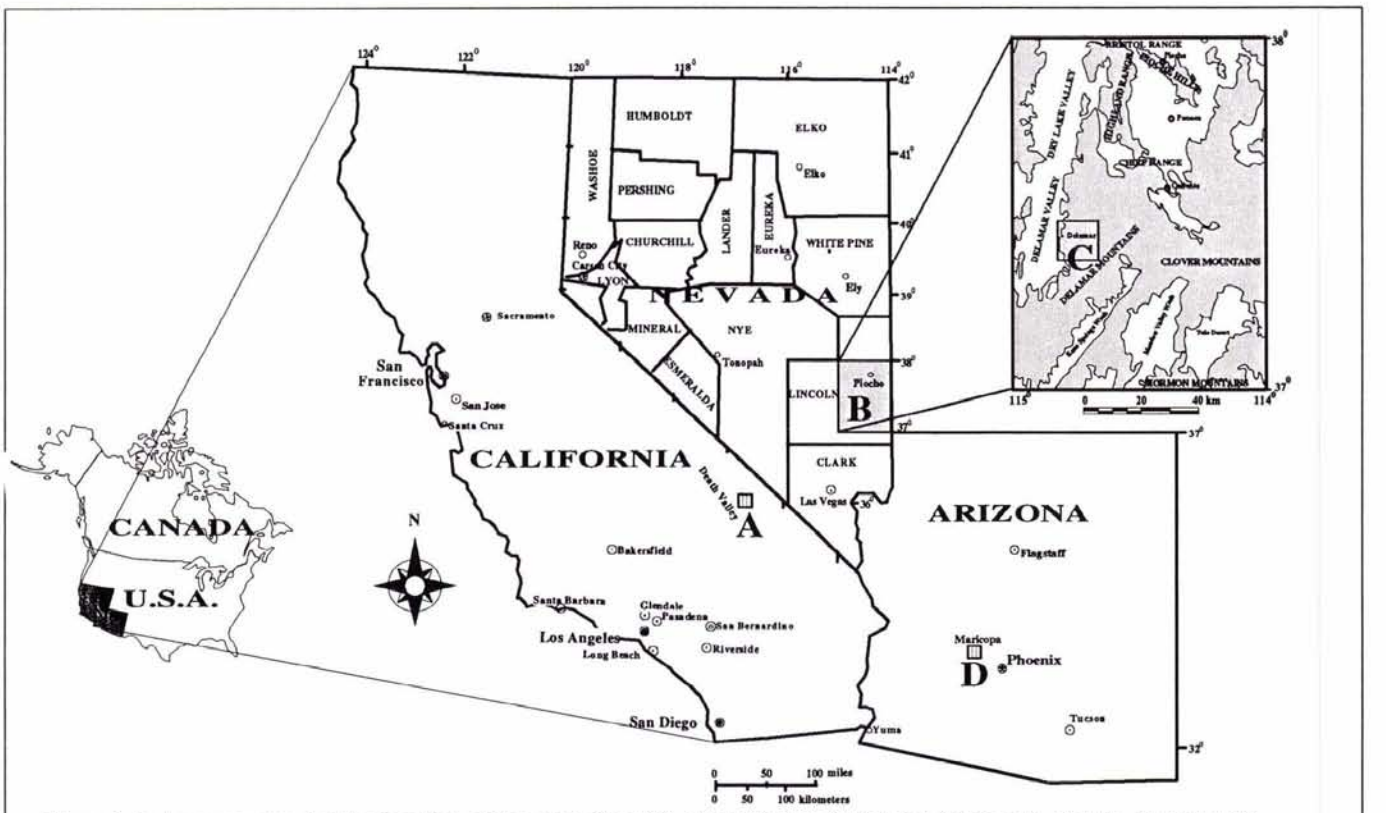

Figure 1. Index map showing the location of the test sites: (A) Death Valley, California; (B) Lincoln County, Nevada; (C) Delamar, Nevada; and (D) Maricopa, Arizona.

shown only statistically. (4) The algorithms assume the data are normally distributed, although this is rarely the case.

The nPDF procedure (Cetin, 1990; Cetin and Levandowski, 1991), which overcomes many of the problems described above, can be conceptualized as a projection of multi-dimensional data onto selected two-dimensional planes (see Appendix 1 for a mathematical explanation of the calculation of the nPDF components.) Most image processing packages include a routine to show the bispectral frequency distributions: the frequency of occurrence of each combination of DN values in a scene. Now assume we have a three-band multispectral digital image. Because the frequency data are three-dimensional and form a data cube (see Figure 3), a conventional image processing package would generate a total of three bispectral frequency plots. These views are perpendicular to the faces of the cube, and for our three-dimensional data there are three unique views (the other three sides of the six cube faces are simply mirror images of the first three). Thus, even in this simplest of cases, with only three dimensions, the image analyst is expected to form a mental synthesis of the overall data distribution from three separate graphs.

Clearly, to form an adequate view of the data distribution, we need a three-dimensional model which we can rotate on the video monitor. Although this can be implemented, we are obviously back to square one if we increase our spectral range to four-dimensional data. Thus, a better strategy is to view the data from selected corners of the data space, a procedure that can be generalized to any number of dimensions. In the case of our hypothetical three-dimensional data, we might, for example, find it useful to look at the data from the corner which corresponds to the origin (i.e., 0 DN) in band 1, and the maximum value (i.e., DN 255) for the other two bands (Corner 4 on Figure 3.) Although this view of the data frequency distribution is only two-dimensional, unlike the bispectral plot projection, it gives a view of all the bands simultaneously. Furthermore, because remote sensing data are typically highly correlated and rarely use the entire potential range of data combinations, we do not necessarily need multiple projections to gain insight into the data distribution.

An efficient and conceptually elegant method of calculating these perspectives is to calculate how far, in DN units, each data frequency point lies from one of the corners of the cube. In Figure 3, for example, we can estimate the position of a point in the data frequency space by calculating the distance from that point to corners 1, 2, 3, or 4. These hyper-dimensional distances, which we call nPDF components, are used as the axes of the nPDF frequency plots. These plots provide an excellent perspective of the data distribution, even in the case of very high dimensional data, such as AVIRIS (see section on classification.)

Frequency plots of two nPDF components (hyper-dimensional distances) provide an excellent perspective of the multi-dimensional data distribution. Ignoring complimentary corners, there are six possible combinations of two corners from which to view the data distribution (1-2, 1-3, 1-4, 2-3, 2-4, and 3-4.) Depending on the spectral distribution of the classes of interest, the user can select corners which provide the maximum separation of the classes.

The cube model has the advantage of being a conceptually simple way of describing corners in multi-dimensional

Figure 2. Index map showing the location of the Quetico test site.

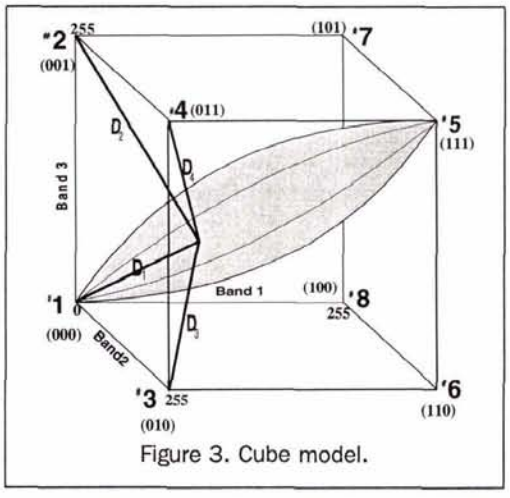

Figure 3. Cube model.

space. However, it does tend to limit the choice of corners for four- and higher-dimensional data. Where this is a problem, we use the "*a*" values (see Equation 1 in Appendix) to describe the corner location. Thus, in Figure 3, corner #2 is also labeled (001), which can be interpreted as a corner that is the minimum for the first two bands, and the maximum in the third band. Using this convention, the length of the list of "*a*" values depends on the number of input bands; thus, the corner corresponding to the origin (corner #1) in a four-band image would be described as (0000).

The nPDF approach to data processing involves more than simply investigating data distributions. First, by transforming the original spectral data into new nPDF hyper-spectral distance bands, the procedure can be used for data visualization and enhancement. In addition, nPDF component plots provide a powerful tool for multispectral image classification. nPDF is, therefore, an integrated, user-interactive approach to image analysis.

Data Visualization

The first stage of data analysis often involves data visualization. In remote sensing, this is usually carried out by viewing the data as an image, typically a false-color composite. However, a conventional false-color composite can only display three bands at a time, and therefore has limited value for high dimensional data such as TM, and especially AVIRIS. One solution is to use Principal Component Analysis (PCA) to transform the data into new bands such that most of the original image variance is present in the first few output bands. Paradoxically, the major disadvantage of PCA is that, as the number of bands increases, and the value of carrying out such a procedure grows, run-times may be so long as to make the procedure prohibitively slow. In addition, the resulting image becomes more and more difficult to interpret.

Another disadvantage of PCA is that it is scene dependent, and is heavily affected by noise present in the data.

An alternative approach is based on the nPDF image processing technique, and overcomes the problems of Principal Component Analysis outlined above. In nPDF data transformation, output bands are calculated by determining the hyper-spectral distance from each pixel to selected corners in the data space using Equation 1 (see Appendix.) Thus, each new output pixel has a DN value determined by how far that pixel lies from the particular corner in the data space that the analyst chooses.

These nPDF transformation images may also be combined in a false-color composite to provide a good perspective of the overall variation in a multi-band image, for example, an AVIRIS or TM scene. The approach works particularly well for TIMS data, where standard false-color composites of radiance data are typically lacking in color variations. Unlike a decorrelation stretch (Plate 1a) of TIMS radiance data (Gillespie *et al.*, 1986), the nPDF procedure does not tend to enhance noise in the data, and can display information from all six TIMS bands in one image (Plate 1b.)

Although there are many possible corners to choose from, we find that two or three corners generally are sufficient to display most of the relationships in TM and TIMS data. The procedure is very fast, making it possible to experiment, and rapidly find three bands that make an effective false-color composite. Obviously, this experimentation can be random, but with even a minimal knowledge of the shape of the spectral curves of the classes in the scene, one can choose corners to highlight particular relationships in the data. For example, an output band calculated from the corner corresponding to the origin in all bands is equivalent to an albedo image. An output band calculated from the corner representing zero in all bands ($a = 0$), and the maximum ($a = 1$) in a selected band, will enhance cover types that have absorption features in the selected band. Furthermore, each output pixel is calculated independently and thus the results are scene independent, unlike a principal component transformation.

Data Enhancement

The nPDF approach can be used to enhance features of interest in transformed bands (Cetin and Levandowski, 1991; 1992.) In order to achieve this, the analyst needs to select the values of the variable "a" in Equation 1 (see Appendix) based on the spectra of the classes of interest. If the original DN values for the class of interest are higher than the other classes in band j, the variable a_j should be set to 0 (in this case, the original DN value of the class is used in Equation 1.) Alternatively, if the class of interest has comparatively low DN values in band j, a_j should be set to 1 (this time the original DN value of the class is subtracted from the maximum DN value, 255 for this study, to obtain a higher output value.) When the summation is performed, the transformed band value will tend to be highest for the class of interest. This enhancement approach is, thus, a maximization technique. The procedure is then repeated for each class.

Three classes, A, B, and C, with hypothetical spectral values (Figure 4) are used to show how this technique works. Let us assume that we want to have high values for the classes A, B, and C in output bands y_1, y_2, and y_3, respectively. For the output band y_1, a_j should be set to 0 for all the four input bands because the class A has the highest value in all the input bands. When the summation is performed and divided by the square root of number of bands (assuming S = 2^{BIT}), the class A will have the highest value (60) compared to the other classes, B (43) and C (42), in the output band y_1 (Table 1.)

We want to have high values for the class B in the output band y_2; therefore, a_j should be set to 0 for the input bands 1 and 3, and a_j should be set to 1 for the input bands 2, and 4 since the class B has higher values in the input bands 1 and 3, and lower in the input bands 2 and 4 compared to the class C. Similarly, for the output band y_3, where we want to have higher values for the class C, a_j should be set to 0 for the input bands 2 and 4, and a_j should be set to 1 for the input bands 1 and 3. Table 1 illustrates how the process results in enhancement of classes A, B, and C in output bands y_1, y_2, and y_3, respectively. When an RGB color combination for the output bands (y_1 = red, y_2 = green, and y_3 = blue) is used, the classes A, B, and C will be seen as red, green, and blue, respectively. The mixed pixels will be seen as the combination of the colors (for example, mixture of the classes A and B will be enhanced as yellow, mixture of all classes will be seen as white, etc.) Landsat TM data of Delamar area in Lincoln County, Nevada were used to illustrate the application of the enhancement technique (see section on classification of diverse data.)

Classification

In addition to data visualization and enhancement, the nPDF approach may also be applied to both supervised and unsupervised classification. A major advantage of nPDF classification is that it is based on an approach to classification quite unlike that of traditional classifiers, and therefore avoids many of their problems. For instance, most traditional approaches are relative classifiers that require all spectral classes to be identified prior to classification, without providing any reliable method of checking that this has been achieved. By contrast, nPDF is an absolute classifier, it is extremely fast, and it can use an unlimited amount of input bands. The procedure utilizes the power of its data visualization capabilities so that the analyst is given a clear depiction

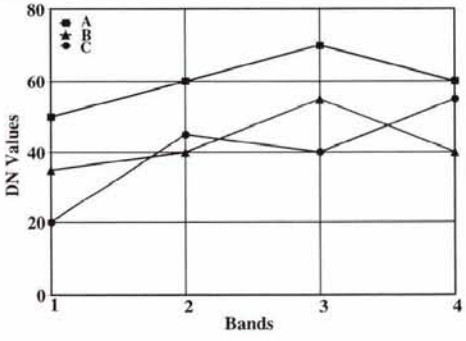

Figure 4. Hypothetical reflectance curves.

TABLE 1. HYPOTHETICAL DN VALUES FOR THREE COVER TYPES AND THREE BAND OUTPUT DATA.

	Input Bands				Output Bands		
Class	1	2	3	4	y_1	y_2	y_3
A	50	60	70	60	**60**	144	144
B	35	40	55	40	43	**155**	151
C	20	45	40	55	42	147	**163**

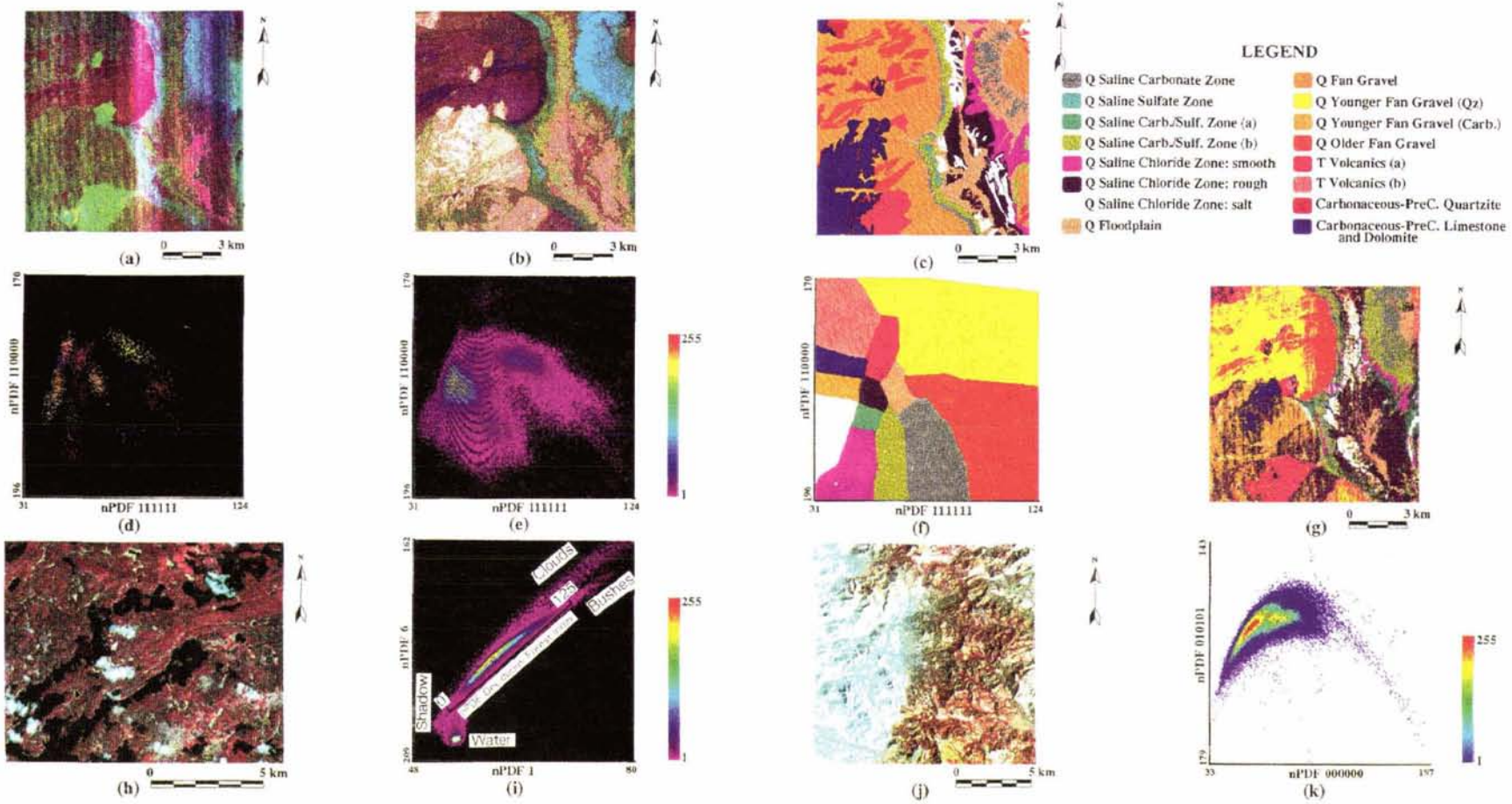

Plate 1. **Death Valley**: (a) False-color composite (red = 8.3, green = 9.1, blue = 9.2) of decorrelation stretched TIMS data. (b) False-color composite (r = NPDF 000000, g = NPDF 000111, b = NPDF 101010) of NPDF transformation of the TIMS data. (c) Geology map of the area. (d) NPDF plot of training data. (e) NPDF plot of entire scene. (f) NPDF look-up table. (g) NPDF classification of the area.
Quetico: (h) False-color composite of TM data. (i) NPDF plot of TM data and location of NPDF Deciduous Forest Index trend.
Delamar: (j) False-color composite of TM data. (k) NPDF plot of entire scene.

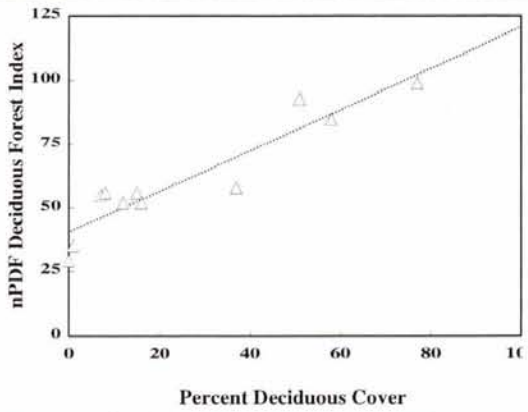

Figure 5. Graph of the average nPDF Deciduous Forest Index versus the percent of the total basal area of the forest community contributed by deciduous species.

of the relationship between the data distribution and the class boundaries.

In the following sections, the nPDF classification technique is explained using TIMS data of Death Valley, California. This is followed by a TM example, where the relative percentages of two classes within each pixel is recovered. nPDF classification is also used to investigate the appropriate window size in gravity and magnetics correlation analysis. Because geological classifications are notoriously subjective, we evaluate the comparative accuracy and speed of the procedure with a classification of agricultural fields, using AVIRIS data of southern Arizona.

Classification of Discrete Classes

Death Valley TIMS data, imaged on 22 July 1983 at 18:43 GMT, were converted to radiance physical units (Palluconi and Meeks, 1985), and then used to estimate surface emittance using the optimum band selections procedure (Warner and Levandowski, 1990.) For visual analysis of the imagery, the radiance data were also converted into nPDF transformation images (see section on data visualization) for display as a false-color composite (Plate 1b.) This false-color composite was compared to a geological map (Plate 1c) of the area (Hunt and Mabey, 1966), and training fields representing 15 different spectral geological classes were chosen.

The emittance data for the 15 training fields were displayed in nPDF plots, using "*a*" values of (111111) and (110000) for the two axes (Plate 1d.) This plot shows that some classes, such as the Quaternary Older Fan Gravel, have a distinct signature. By comparison, as might be expected, the Limestone and Dolomite is rather poorly separated from Younger Fan Gravel (Carbonate.) Finally, there are cover types that are not separable at all. Three such classes of the original 15 training fields in Death Valley were merged with other classes, leaving the 12 classes shown in Plate 1d. When the entire emittance data set is also plotted in the same nPDF space (Plate 1e), and compared to the training data distribution, it can be seen that the 12 classes cover most of the spectral distribution of the original scene. However, note that the classes in the training data do not adequately cover the spectral distribution along the bottom edge of the scene distribution (Plate 1e.)

For classification, the analyst overlays the nPDF plots of the data and training field distribution on the computer monitor, and then digitizes the boundaries of the classes the analyst wishes to identify. In Plate 1f, a thirteenth class has been digitized to represent the unknown class. The digitized regions are then converted to a lookup table, which is used to classify the entire image. At this stage the unknown class was identified as a spectrally distinct unit within the Saline Carbonate/Sulfate zone, by comparing the final classified image to the geological map (Plate 1g.)

Classification of Mixtures

The TIMS Death Valley application demonstrates the procedure of standard classification, where it is desired that the scene be classified into discrete classes. In some cases, however, the classes of interest are mixed at the sub-pixel scale. For example, in a geobotanical study of Quetico Provincial Park, Ontario, the percentage of deciduous trees in a mixed coniferous - deciduous forest was found to increase in greenstone areas, compared to the surrounding granites (Warner *et al.*, 1991; Warner *et al.*, 1993). Thus, it is the relative mixture of deciduous and coniferous trees, rather than the identification of discrete classes, that is of interest in this area. The TM data (Plate 1h) was imaged on 21 August 1986.

Plate 1i shows the nPDF spectral distribution of the TM scene, and the figure has been annotated to indicate the informational classes. Note that in this example the axes are numbered by the convention of a hyper-spectral cube (see Figure 3.) Using ground reference data, a forest trend is identified in the nPDF spectral plot, and the entire scene is transformed to a new nPDF Deciduous Forest Index, with a value of 0 for the most coniferous pixels, and 125 for the most deciduous. This transformation is carried out in a manner analogous to the nPDF transformations described for the TIMS data in the section on data visualizations. In this case, however, the transformation is along a line identified in the nPDF spectral distribution plot, instead of simply representing a distance to a corner. Non-forested areas are separately classified, thus demonstrating the advantage of nPDF as an absolute classifier in which only the classes of interest need be identified.

The validity of the transformation was checked using 11 field surveys, which were located randomly throughout the study area. The surveys were carried out using the standard forest mensuration technique of polyareal plot sampling (Husch *et al.*, 1982) with the aid of a 9.3 factor prism. In this way the proportion of each species as a percentage of the total cross-sectional area of tree trunks in the measured forest stand was determined. In the relatively even-aged forests of Quetico, there are few understory trees. Thus, this proportional tree trunk-based measurement provides a surrogate estimate of the relative dominance of each species in the forest canopy imaged from above by the satellite. Although these field data are rather limited, Figure 5 suggests that the average nPDF Deciduous Forest Index determined from the TM data shows an excellent linear relationship with the percent deciduous cover identified in the field survey.

Classification of Diverse Data

Landsat TM data of Delamar area in Lincoln County, Nevada were used to illustrate enhancement and classification for mapping hydrothermally altered zones. The Delamar area is underlain by Cambrian and Tertiary rocks, with most mineralization occuring in the Cambrian section. Hydrothermal alteration in this area is very extensive at the surface and centers around the Delamar mine (Ekren *et al.*, 1977.) The rocks in the area are altered largely to argillic mineral assemblages. Iron staining is also common.

A small block of training pixels for each of three cover types was selected from the Delamar TM scene (Plate 1j) (Cetin and Levandowski, 1992): mine tailings, hydrothermal alteration, and vegetation (see Table 2.)

As seen from Table 2, original DN values for the mine tailings class are higher in all bands than the other classes. Therefore, a_j in Equation 1 was set to 0 for all input TM bands to enhance the mine tailings class in output band 1. The hydrothermal alteration class has low DN values in bands 2, 4, and 7, but high DN values in bands 1, 3, and 5. By contrast, the vegetation class has the opposite character: low in bands 1, 3, and 5, high in bands 2, 4, and 7. Thus, for output band 2, in which the hydrothermal alteration is desired to have higher values, a_j was set to 1 for the input bands 2, 4, and 7; and was set to 0 for the input bands 1, 3, and 5. Similarly, for output band 3, for which it is desired that vegetation has the highest values, a_j should be set to 0 for the input bands 2, 4, and 7; and a_j should be set to 1 for the input bands 1, 3, and 5. The calculation results (output band values) using the a_j values are given in Table 2. As seen from Table 2, the classes mine tailings, hydrothermal alteration, and vegetation are enhanced in output bands y_1, y_2, and y_3, respectively. The resultant data with three bands were displayed using red color for band 1 (y_1), green for band 2 (y_2), and blue for band 3 (y_3.) This false-color composite successfully displayed altered areas in green.

The maximization image above demonstrates that "a" values of (000000) and (010101) produced an effective enhancement of the cover classes of mine tailings and hydrothermal alteration. These same "a" values are, therefore, the most appropriate for image classification. The nPDF data distribution shows that there are three clusters in the data (Plates 1k and 2a.) Analysis of the training data shows that these clusters are associated with (from left to right in Plate 1k) vegetation, clay alteration, and mine tailings (Plate 2b.)

The nPDF classification was also used to support the analysis of geophysical correlations for Lincoln County, Nevada. The entire study area is 110 kilometers (east-west) by 160 kilometers (north-south) in extent. Gravity (Plate 2c) and reduced-to-the-pole magnetic data were co-registered to the same Universal Transverse Mercator (UTM) grid. The magnetic (Plate 2d) data were compiled at 2,740 meters, and therefore the gravity data were upward continued to this level. Both data sets were also upward continued to the 5,000- and 7,000-metre levels. For each level, the first derivative of the gravity was then calculated. Correlation analysis was then performed on the three levels of gravity and magnetics data, using window sizes of 3, 5, and 9 kilometers. Graphs of the nPDF data distribution for each of these analyses showed that the window size of 9 kilometers gave the best result, with the most geologically significant clusters in nPDF space (see Plate 2e.)

Comparative Accuracy and Speed

Classification accuracy may best be evaluated in areas of comparatively uniform cover, such as the AVIRIS scene (Plate 2f) of 4 October 1990, which covers southern Arizona. For comparison of nPDF to traditional classifiers, we were limited to no more than 15 bands, as that is the maximum allowed by the image processing software used (ERDAS, 1990.) By contrast, nPDF classification and analysis can use a virtually unlimited number of bands. For example, 180 bands of AVIRIS data were used in an nPDF classification. The nPDF analysis of a small test site (Plate 2g) within this scene followed the procedure outlined for the classification of discrete classes (Plate 2h.) As discussed previously, training fields for the discrete classes were mapped into the nPDF spectral space (Plate 2k.) Plate 2i shows the nPDF plot of AVIRIS data and Plate 2j shows the nPDF plot of the test site. A look-up table using the training data distribution was created, and the test site was classified using the supervised nPDF classification (Plate 2l.) The results of this, and more traditional classifications, are compared in Table 3, which is based on detailed ground information(Plate 2h.) nPDF had the highest overall accuracy rate, 71 percent, compared to 53 percent for minimum distance, 67 percent for maximum likelihood, and 68 percent for Mahalanobis distance.

The nPDF technique is also very fast. Figure 6 shows that the run-times of the traditional techniques are several times longer than nPDF, and that for the Mahalanobis distance and maximum-likelihood classifiers, run-times increase exponentially with the number of bands. Furthermore, the nPDF classification is unaffected by the number of classes (Figure 7), whereas the run-time for minimum distance increases linearly with the number of classes, and for the remaining classifiers the increase is approximately exponential.

TABLE 2. AVERAGE DN VALUES FOR THREE AREAS OF KNOWN COVER TYPE IN THE DELAMAR, NEVADA TM SCENE AND THREE BAND OUTPUT DATA USING THE ENHANCEMENT (MAXIMIZATION) TECHNIQUE.

	Input TM Bands (DN values)						Output Bands		
Class	1	2	3	4	5	7	y_1	y_2	y_3
Mine Tailings	120	70	85	100	160	89	**108**	149	115
Hydrothermal Alteration	100	55	60	65	120	35	78	**159**	122
Vegetation	95	60	50	80	70	40	68	148	**138**

TABLE 3. CLASSIFICATION ACCURACY PERCENTAGES.

Cover Class	Maximum Likelihood	Mahalanobis	Minimum Distance	nPDF
Cotton 1	99.1	98.7	92.3	95.7
Cotton 2	41.3	45.0	53.2	59.6
Cotton 3	59.7	62.0	50.3	59.6
Cotton 4	98.3	98.0	56.9	99.0
Alfalfa	80.9	83.4	33.4	83.5
Grapes	79.5	77.6	65.0	85.3
Bare Soil	79.6	77.6	70.8	85.3
Wheat Stubble	64.6	66.4	55.4	65.9
Overall	**67.3**	**67.8**	**52.7**	**71.0**

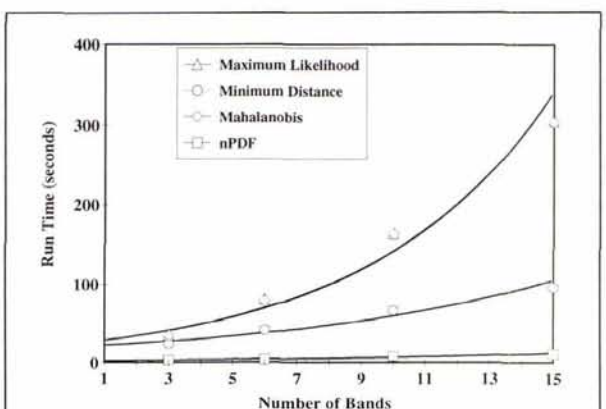

Figure 6. Effect of number of bands on classification run time.

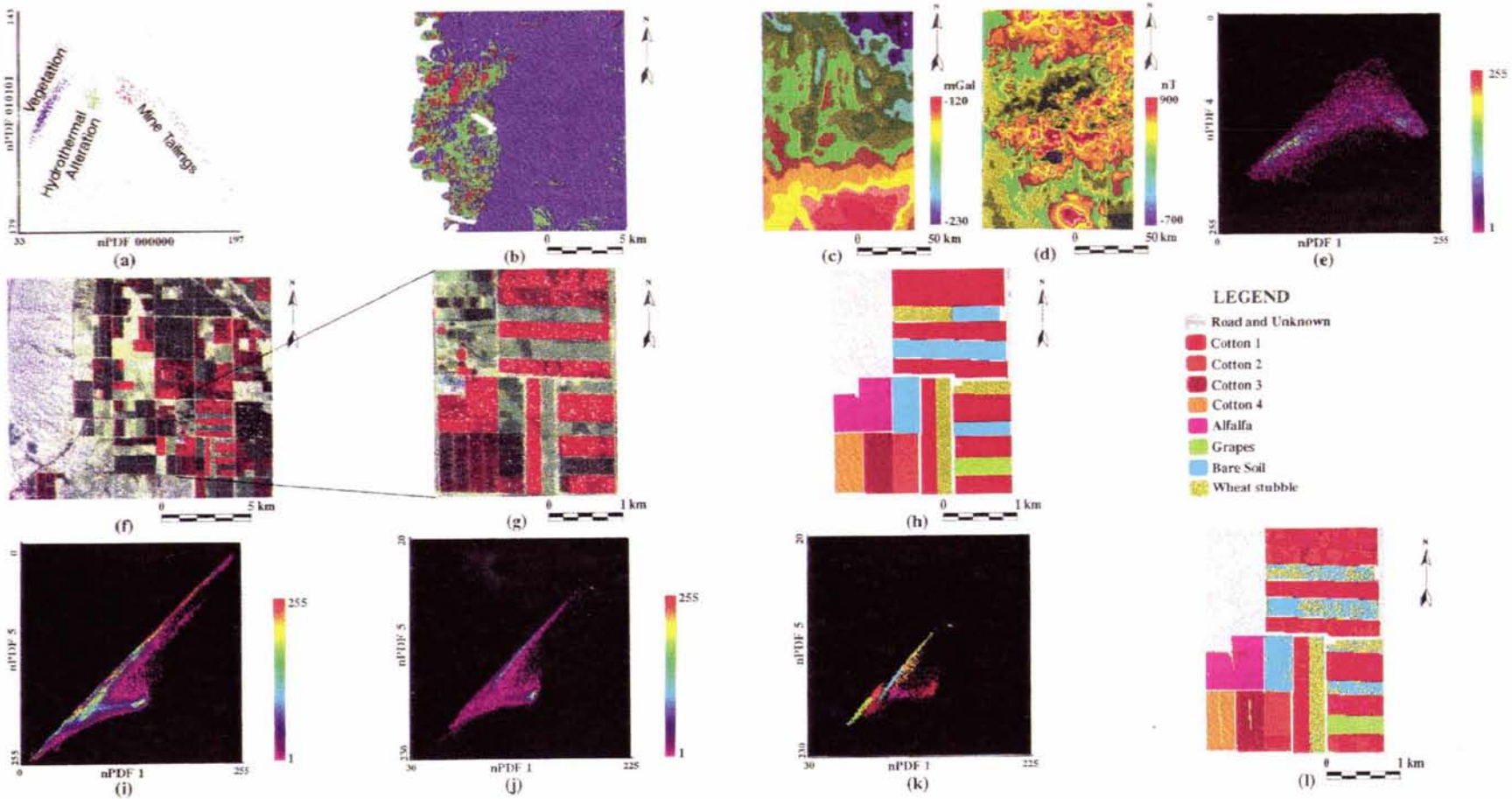

Plate 2. **Delamar**: (a) nPDF[h] plot of training fields. (b) nPDF classification of the area.
Lincoln County: (c) Color coded gravity data. (d) Color coded magnetic data. (e) nPDF distribution of combined gravity and magnetic data at 2470, 5000, and 7000 metres with a window size of 9 kilometres.
Maricopa: (f) False-color composite of AVIRIS data. (g) False- color composite of AVIRIS data of the test site. (h) Ground information of the test site. (i) nPDF plot of the AVIRIS data. (j) nPDF plot of the AVIRIS data of the test site. (k) nPDF plot of training data of the test site. (l) nPDF classification of the test site.

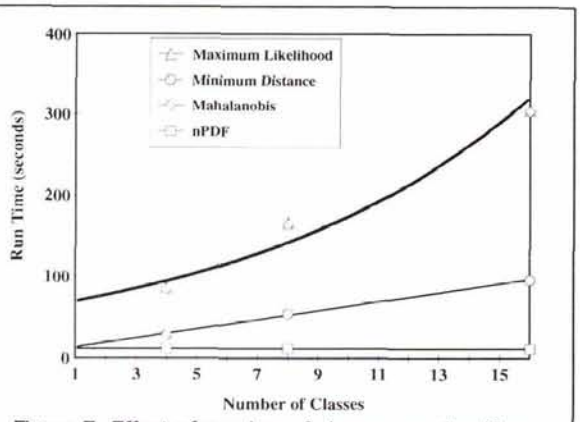

Figure 7. Effect of number of classes on classification run time.

To demonstrate the power of the nPDF approach, the entire AVIRIS scene of 512 lines by 614 pixels with a total of 180 bands, representing over 56 megabytes of data, was classified using the Maricopa training information. This entire classification took 12 minutes and 48 seconds using a Northgate 25 megahertz 486 computer.

Summary

The nPDF approach provides a complete procedure from data visualization, to enhancement and classification. In a typical analysis these steps all support each other. The classification relies on data visualization techniques, and may incorporate data enhancements. It is the opposite of a "black box" approach: the spectral and informational class distributions are presented in graphical form and the nature of transformations, data perspectives, and spectral classes may be investigated by producing nPDF plots and transformations of the original data. In an unsupervised classification, the nPDF plot of the spectral distribution provides information as to the best estimate of the number and starting locations of the means for the clusters. For supervised classification the relationship between the spectral information in the entire scene and the informational classes is clearly presented. Mixtures can be classified, for example, into the proportion of deciduous vegetation in a mixed deciduous-coniferous forest. nPDF analysis also supports complex analyses of geophysical data. The procedure is not only more accurate than conventional classifiers, but also much more rapid.

Acknowledgments

We are very grateful to the scientists who kindly provided the imagery used in this investigation: Elsa Abbott and Ann Kahle of J.P.L., Phil Slater of the University of Arizona, Ray Jackson of U.S.D.A., and Robin Bell of N.A.S.A. This study was supported by the Indiana Mining and Mineral Resources Research Institute and by an A. H. Ismail Interdisciplinary Program Doctoral Research Grant.

References

Cetin, H., 1990. nPDF-An algorithm for mapping n-dimensional probability density functions for remotely sensed data, *Proceedings of the 10th Annual International Geoscience & Remote Sensing Symposium, IGARSS'90*, I:353–356.

Cetin, H., and D. W. Levandowski, 1991. Interactive classification and mapping of multi-dimensional remotely sensed data using n-dimensional probability density functions (nPDF), *Photogrammetric Engineering & Remote Sensing*, 57(12):1579–1587.

———, 1992. A maximization method to map hydrothermal alteration zones using remotely sensed data, *GeoTech'92: Geocomputing Conference*; pp. 397–410.

Ekren, E. B., P. P. Orkild, K. A. Sargent, and G. L. Dixon, 1977. *Geologic Map of Tertiary Rocks, Lincoln County, Nevada*, U. S. Geological Survey Miscellaneous Investigations Map I–1041.

ERDAS, 1990. *ERDAS Version 7.4 User's Manual: Image Processing Module*, Atlanta, Georgia, 218 p.

Gillespie, A. R., A. Kahle, and R. E. Walker, 1986. Color enhancement of highly correlated images. I. Decorrelation and HSI contrast stretches. *Remote Sensing of Environment* 20:209–235.

Hunt, C. B., and D. R. Mabey, 1966. *Stratigraphy and Structure of Death Valley, California*, U.S. Geological Survey Professional Paper 494–A, 162 p.

Husch, B., C. I. Miller, and T. Beers, 1982. *Forest Mensuration, Third Edition*, John Wiley and Sons, New York, New York, 402 p.

Palluconi, F. D., and G. R. Meeks, 1985. *Thermal Infrared Multispectral Scanner (TIMS): An Investigators' Guide to TIMS Data*, JPL Publication 85–37, Pasadena, California, 24 p.

Warner, T. A., and D. W. Levandowski, 1990. Optimum band selections for estimating emittance from TIMS data, *Proceedings of the second Thermal Infrared Multispectral Scanner (TIMS) Workshop* (Abbot, E. A., editor), 6 June 1990, JPL Publication 90–55, pp. 31–35.

Warner, T. A., D. J. Campagna, C. S. Evans, D. W. Levandowski, and H. Cetin, 1991. Analyzing remote sensing geobotanical trends in Quetico Provincial Park, Ontario, Canada, using digital elevation data, *Photogrammetric Engineering & Remote Sensing*, 57(9):1179–1183.

Warner, T. A., D. W. Levandowski, R. Bell, and H. Cetin, 1993. Topoveg: A rule based geobotanical program to classify aeromagnetic, topographic and remotely sensed vegetation community data, *Proceedings of the Ninth Thematic Conference, Geologic Remote Sensing*, I:345–356.

Appendix

The nPDF approach may be explained using a cube model (Cetin and Levandowski, 1991.) A generalized distribution of highly correlated digital remotely sensed data in three-dimensional feature space is shown in Figure 3. In three-dimensional feature space the feature vector is defined by $X=[x_1,x_2,x_3]$. The location of a point within the range of the total possible measurement space can be described by the distances to the two corners of the cube shown in Figure 3. They are

$$D_1 = [x_1^2 + x_2^2 + x_3^2]^{1/2} \text{ and } D_2 = [x_1^2 + x_2^2 + (R - x_3)^2]^{1/2}.$$

For the multi-dimensional case, the feature vector is defined by $X=[x_1,x_2,x_3,\ldots,x_n]$, where n is the dimension of the data and R is the maximum possible range of the data (255 for 8-bit data.) When a hyper-dimensional cube is used, the vector magnitudes (the distances to the two corners) for n-dimensional data are

$$D_1 = \left(\sum_{j=1}^{n} x_j^2 \right)^{1/2}$$

$$D_2 = \left(\sum_{j=1}^{n} x_j^2 * (1 - a_j) + (R - x_j)^2 * a_j \right)^{1/2}$$

$$\text{if} \begin{cases} j = 1,2,4,5,\ldots & a = 0 \\ j = 3,6,\ldots & a = 1 \end{cases}$$

where j is the band number. A generalized formula for the

distance to the corners of a hyper-dimensional cube can be written as (i is the corner or component number)

$$D_i = \left(\sum_{j=1}^{n} x_j^2 * (1 - a_j) + (R - x_j)^2 * a_j \right)^{1/2} \quad (1)$$

There are eight possible corners of a three-dimensional cube as is shown in Figure 3. Four of the corners can be selected as principal corners (1 through 4); the remaining corners (5 through 8) are complimentary to the four principal corners. For the hyper-dimensional cube model, "a" values for Equation 1 are as follows (j is the band number):

D_1 : For all j values $a = 0$

$$D_2 : \text{if } \begin{cases} j = 1,2,4,5,\ldots & a = 0 \\ j = 3,6,\ldots & a = 1 \end{cases}$$

$$D_3 : \text{if } \begin{cases} j = 1,3,4,6,\ldots & a = 0 \\ j = 2,5,\ldots & a = 1 \end{cases}$$

$$D_4 : \text{if } \begin{cases} j = 1,4,\ldots & a = 0 \\ j = 2,3,5,6,\ldots & a = 1 \end{cases}$$

The nPDF formula is

$$\text{nPDF}_i = S * D_i / (2^{\text{BIT}} * \text{NB}^{1/2}) \quad (2)$$

where

nPDF_i = component i of nPDF,
i = corner number,
S = desired scale for the nPDF axes,
D_i = calculated distance for component i,
BIT = number of bits of input data, and
NB = number of bands used.

A convenient scale for these nPDF components is 8 bit in range, and thus a two-dimensional frequency plot requires a 256 by 256 array.

REMOTE SENSING & NATURAL RESOURCE MANAGEMENT

Proceedings of the Fourth Forest Service Remote Sensing Applications Conference 6-11 April 1992

1992. 456 pp. $75 (softcover); ASPRS Members $40. Stock # 4532.

The Forest Service Remote Sensing Applications Conference provides an arena for resource managers to share information and learn about new technology and new applications that can help manage our nation's natural resources. The conference has continued to grow and expand to include more participants from forests and districts throughout the country, other government agencies, universities and private companies and organizations. This text contains the papers of the fourth such conference which was held in Orlando, Florida.

Topics include:

- Digital Image Analysis Techniques on an IBM Microcomputer for Measuring Soil Disturbance Following Timber Harvesting
- Forest Species and Structure Analysis Using a Hyper-Spectral Scanner (AVIRIS) and Terrain Normalization Algorithms
- Three-Dimensional Terrain Visualization with a Real-Time Interface to a Photographic Stereomodel
- Applications of GPS/GIS for Fire Mapping in Everglades National Park
- The Use of GPS, GIS, and Remote Sensing in a Stratified Forest Survey
- Real-Time Differential GPS: An Aerial Survey—Remote Sensing Application
- Aerial Video and Associated Technologies for Forest Assessments

For details on ordering, see the ASPRS store in this journal.